JOURNAL OF RESEARCH of the National Bureau of Standards—D. Radio Propagation

Vol. 64D, No. 4, July–August 1960

Daytime Attentuation Rates in the Very Low Frequency Band Using Atmospherics*

W. L. Taylor

(January 25, 1960)

Daytime attenuation characteristics have been computed by comparing the amplitude spectra of atmospheric waveforms recorded at four widely separated stations. The results of these attenuation measurements are presented for the band of frequencies from 3 to 30 kilocycles per second and involving distances of 1,000 to 10,000 kilometers. It was found from these data that attenutation was about 7 to 9 decibels per 1,000 kilometers at 6 kilocycles per second and decreases to about 1 to 3 decibels per 1,000 kilometers at frequencies greater than 10 kilocycles per second. The difference in attenuation rate of west-to-east propagation relative to east-to-west propagation was about 3 decibels per 1,000 kilometers less for frequencies lower than 8 kilocycles per second and about 1 decibel per 1,000 kilometers less from frequencies higher than 10 kilocycles per second.

1. Introduction

Considerable electromagnetic energy is radiated into the atmosphere from lightning discharges. These signals are referred to as atmospherics. The spectra of signals from return stroke lightning discharges attain a peak in the VLF region, usually between 5 and 20 kc. The radiation field spectra near the source are relatively broad i.e., 10 to 15 kc between the frequencies at which the spectral amplitude is 3 db below the peak amplitude. As the propagation distance increases, the spectra begin to narrow such that at distances greater than a few thousand kilometers the spectral width is only 3 to 5 kc. The spectra of atmospherics simultaneously recorded at several locations can be analyzed to determine the attenuation rates as a function of frequency and direction.

Many recent experimental and theoretical investigations have been conducted for purposes of better understanding VLF propagation characteristics.[1] The objective of this paper is to present the results of a study of daytime attenuation rates at VLF using atmospheric waveforms recorded at four widely separated locations.

2. Theoretical Considerations

The Fourier spectrum of an electromagnetic pulse can be represented by the integral

$$E(\omega,d)=\int_0^\infty G(t,d)\cdot e^{-i\omega t}dt \tag{1}$$

where ω is the angular frequency $(2\pi f)$; d is the distance in kilometers; t is the time in seconds, and $G(t,d)$ is the instantaneous value of the vertical component of the electric field. Also

$$G(t,d)=0 \text{ for } t<0 \text{ and } t>\tau \tag{2}$$

where τ is the length of the pulse waveform.

Now (1) can be written

$$E(\omega,d)=|E(\omega,d)|e^{-i\phi(\omega,d)}. \tag{3}$$

The function $|E(\omega,d)|$ is the amplitude spectrum and the function $\phi(\omega,d)$ is the phase spectrum as a function of frequency at some distance d. The phase of the spectrum can be used to determine phase velocity of propagation [1].[2] Only the amplitude value, $|E(\omega,d)|$, need be considered for purposes of computing attenuation presented in this paper.

Assuming the source is an equivalent dipole, the spectrum of the vertical electric field at a great-circle distance, d, is given by the mode sum

$$|E(\omega,d)|=A(\omega)W, \tag{4}$$

where $A(\omega)$ is the amplitude coefficient dependent upon the spectrum of the source, and W is the resultant of the complex sum of all active waveguide type modes [2 to 4]. It is extremely difficult to evaluate (4) in a practical situation involving present experimental techniques. However, the main contribution to the spectrum is given by

$$|E(\omega,d)|\simeq A(\omega)[a\sin d/a]^{-1/2}e^{-\alpha(\omega)d}, \tag{5}$$

where a is the radius of the earth in kilometers and $\alpha(\omega)$ is the attenuation coefficient in nepers. This relation expresses the dominant term in a mode series representation of the resultant spectrum, and is an equality only when there is one active mode in the waveguide. This condition was approximately met in the present work as it was in previous work [5].

The principal task was to determine the attenuation as a function of frequency. To accomplish this the vertical electric field waveform of the same lightning stroke was recorded at several locations. The Fourier spectrum of each waveform was then

* Contribution from Central Radio Propagation Laboratory, National Bureau of Standards, Boulder, Colo.

[1] A selection of representative references is appended.

[2] Figures in brackets indicate the literature references at the end of this paper.

calculated. Using the subscript i to denote the far station and the subscript j to denote the near station, such that $d_i > d_j$, it follows from eq (5) that

$$\exp\,[\alpha(\omega)\cdot(d_i-d_j)]=\frac{|E(\omega,d_j)|}{|E(\omega,d_i)|}\cdot\left[\frac{\sin\,(d_i/a)}{\sin\,(d_j/a)}\right]^{-1/2}. \quad (6)$$

The attenuation coefficient $\alpha'(\omega)$ expressed in decibels per 1,000 km is given by

$$\alpha'(\omega)=\left[20\log\frac{|E(\omega,d_j)|}{|E(\omega,d_i)|}-10\log\frac{\sin\,d_i/a}{\sin\,d_j/a}\right]\cdot\frac{10^3}{d_i-d_j} \quad (7)$$

where $\alpha'(\omega)=\alpha(\omega)\times 8.68\times 10^3$.

3. Experimental Procedure

3.1. Equipment

The vertical component of the electric field of atmospherics was received using a vertical antenna and wideband receiving equipment. These atmospheric waveforms were displayed on a multigun cathode-ray tube at two sensitivities and recorded on continuously moving photographic film. The amplitude response of the waveform channel was approximately flat throughout the band-pass and sloped to 6-db points at frequencies of 1 and 100 kc. The phase response was essentially linear with frequency within the band-pass. The cathode-ray tube display is proportional to the free-space field incident at the antenna. Included in the vertical electric field channel was a 23-ft vertical antenna, antenna cathode follower, band-pass filters composed of RC networks, a 24-μsec delay line, wideband amplifier, and oscilloscope. The overall characteristics of this channel were adequate to faithfully record the VLF components of atmospheric waveforms.

Calibration was performed by inserting a voltage into a dummy antenna driving the cathode follower, and adjusting amplifier gain to give the desired deflection on the cathode-ray tube. This calibration voltage was equal to the expected field strength times the antenna effective height, assumed to be one-half its physical length.

Amplitude threshold triggering was used to discriminate against the numerous low-amplitude atmospherics. Signals that exceeded a selected amplitude, prior to passing through the delay line, activated the sweep circuit of the oscilloscope. All signals received with the vertical antenna were displayed on the oscilloscope from 24 μsec before to 1 msec after the time when the amplitude of the atmospheric reached the triggering level. Use of the delay line minimized possible loss of the early part of the waveforms.

The direction of arrival of atmospherics was displayed on the same multigun oscilloscope. A pair of vertical electrostatically-shielded loop antennas, arranged at right angles to each other, loop receivers, filters, delay lines, and amplifiers composed the direction-finding system. The overall transfer characteristics of each loop-antenna channel closely approximated that of the vertical-antenna channel. The differences between the amplitude and phase responses of the two loop-antenna waveform channels were less than 0.5 db and 6 deg, respectively, over the entire band-pass.

The direction-finding display on the oscilloscope was activated for approximately 200 μsec at the beginning of each atmospheric. Thus, the direction of arrival was determined from the initial portion of the signal, which is essentially vertically polarized. Accuracy of determining direction of arrival was about $\pm 2°$ for each station.

The time of arrival of atmospherics was determined to and accuracy of about ± 1 msec. This was accomplished by recording on the waveform records the standard time signals from stations WWV (or WWVH) and timing marks from a secondary frequency standard which was synchronized with the seconds "tick" from WWV. The measured arrival times of atmospherics were corrected for propagation time of the signals from the standard time station to the recording site.

Four sets of this equipment were operated simultaneously at Boulder, Colo.; Salt Lake City, Utah; Palo Alto, Calif.; and Maui, Hawaii, on a number of occasions during the summer of 1958. The recording sensitivities and the triggering amplitudes were selected for each station to accommodate atmospherics originating in the western half of the United States. The transfer characteristics of the vertical antenna waveform channel were frequently checked at each station to insure uniformity of responses between stations. It was found that the differences between the response characteristics of the equipment at different stations were less than ± 0.5 db and $\pm 20°$, respectively, in amplitude and phase. These differences are small for the purposes of this paper.

Atmospheric waveforms resulting from a particular lightning discharge were located on the photographic records made of each station by virtue of their times of reception and directions of arrival. The locations of these discharges were determined by triangulation, using the direction of arrival indicated at each station.

3.2. Analysis—East-to-West Propagation

Waveforms from fifty lightning discharges were obtained from the data collected on July 2, 1958, 1900 to 2100 G.m.t.; July 7, 1958, 2300 to 0100 (July 8) G.m.t.; and July 9, 1958, 1900 to 2100 G.m.t. Atmospherics recorded at each of the four stations from twenty of these lightning discharges were analyzed. This analysis consisted of (1) scaling the individual waveforms recorded at each station to determine the functions $G(t, d)$, (see eqs (1) and (2)), (2) computing the complex spectra (eq (1)) every kilocycles per second from 1 to 100 kc, and (3) computing the attenuation (see eq (7)) for each pair of stations, i.e., Boulder—Maui, Salt Lake City—Maui, and Palo Alto—Maui. The distances from the sources of each atmospheric to the near station were between

1,000 to 2,400 km, while the distances from the sources to Maui (the far station) were between 4,160 to 5,200 km. Accuracy of determining the location of the individual atmospherics was about ±10 percent of the distance to the near station.

One set of waveforms, their corresponding amplitude spectrum, and the computed attenuations ($\alpha'(\omega)$), representative of those used in this analysis, are given in the first four figures. The waveforms,

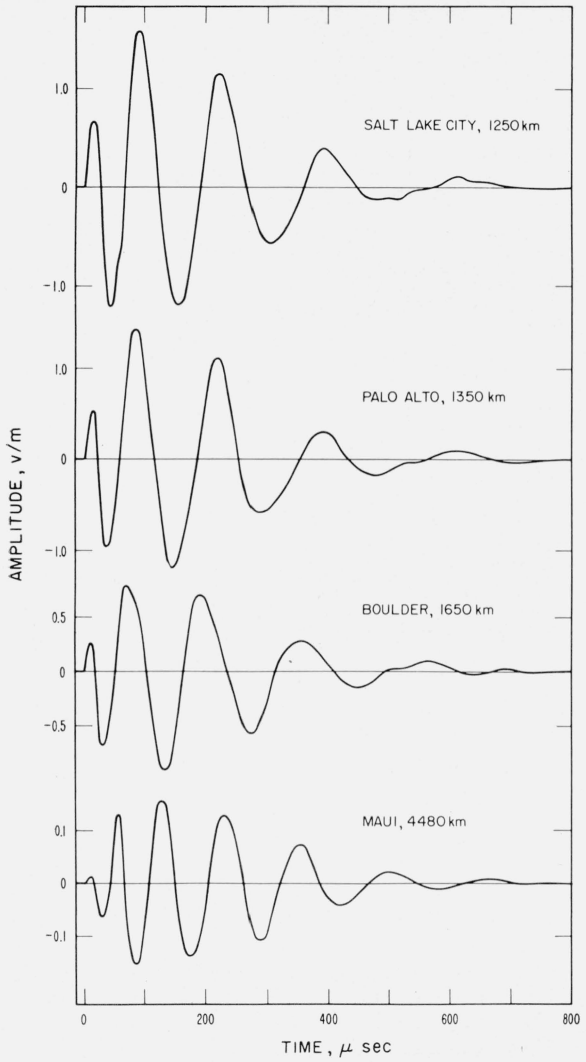

FIGURE 1. *Representative atmospheric waveforms, east to west.*

shown in figure 1, are reproduced on the same time base but different amplitude scales, while the recording stations and the distances to the source are indicated. Note in particular the progression to shorter time intervals of the points where each waveform successively crosses the zero amplitude axis as propagation distance increases. The times in microseconds of these quasi half-periods, presented in figure 2, show clearly the progression to shorter time intervals as propagation distance increases. These values, from the representatives set of waveforms, agree quite reasonably with those found by other

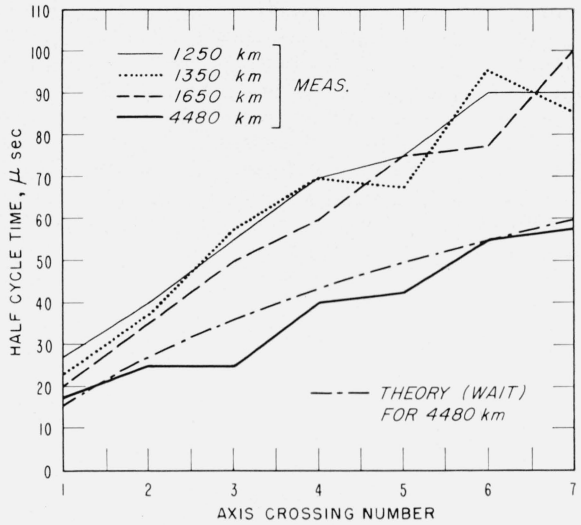

FIGURE 2. *Quasi half-periods of representative atmospherics, east to west.*

workers [6, 7], and the behavior is in accord with theoretical investigation of the phenomenon [8]. Further elaboration concerning the atmospheric wave shapes are beyond the scope of this paper.

The spectra of these atmospherics are presented in figure 3. It should be observed that the frequency of

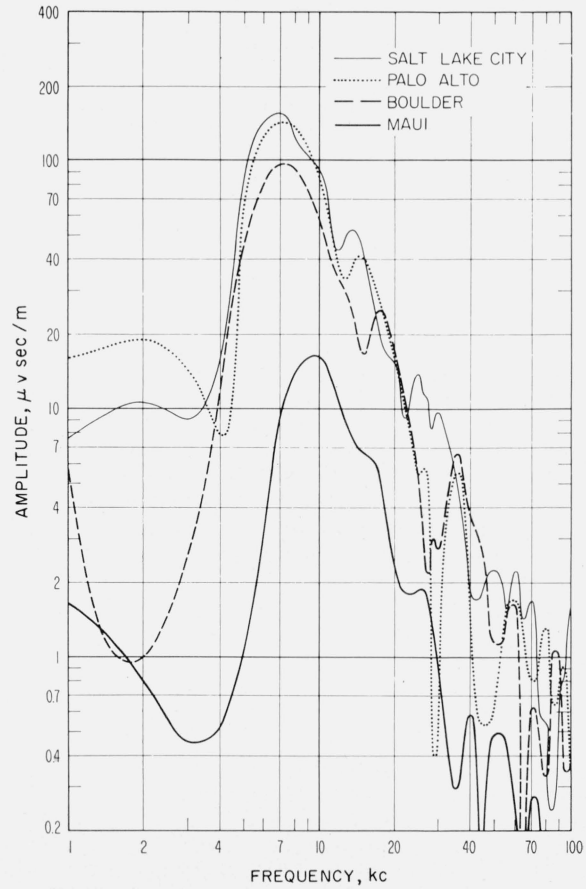

FIGURE 3. *Representative spectra, east to west.*

the peak amplitude of each spectrum is increasing as the propagation distance increases.

The attenuation in decibel per 1,000 km computed from these spectral values are presented in figure 4. Values of attenuation for each frequency from each set of computations, using Boulder to Maui, Salt Lake City to Maui, and Palo Alto to Maui, are in reasonably good agreement. Accuracy of determining differences in distance between each station of a pair and the source was about 7 percent.

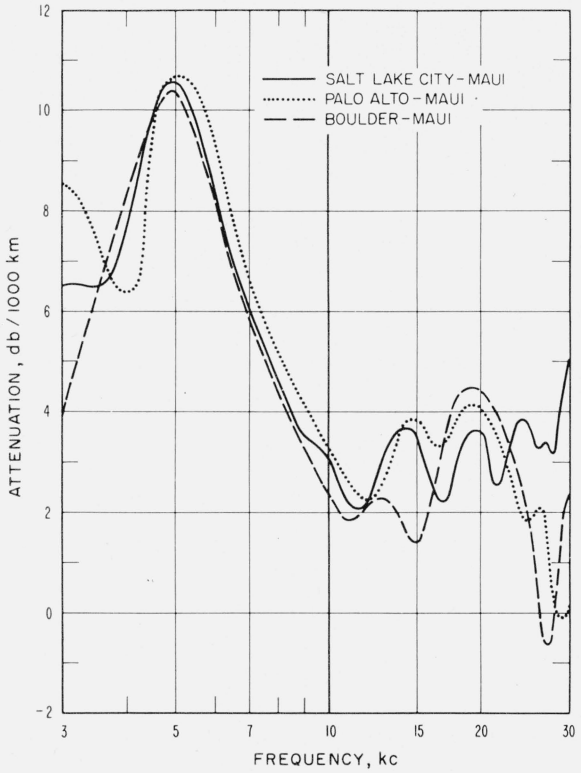

FIGURE 4. *Representative attenuation, east to west.*

Values of the spectral components of frequencies lower than about 4 kc and higher than about 30 kc are relatively small, less than 20 db below the peak spectral value. Errors in the computed attenuation resulting from limitations in the described technique may become large as the amplitude of the spectra approaches very small values. Therefore, computations of attenuation were limited to the VLF region of the spectrum (3 to 30 kc).

The analysis of the waveforms from the other lightning discharges give results similar to the example presented in figures 1, 3, and 4.

Considerable variability was found between the shapes of the attenuation versus frequency curves, obtained from the data recorded at each pair of stations. Six individual curves of attenuation as a function of frequency are presented in figure 5. The curves are identified by capital letters (A) and their corresponding "zero decibel level" by lower case letters (a). The names of the stations and distances from the source in kilometers are given with the

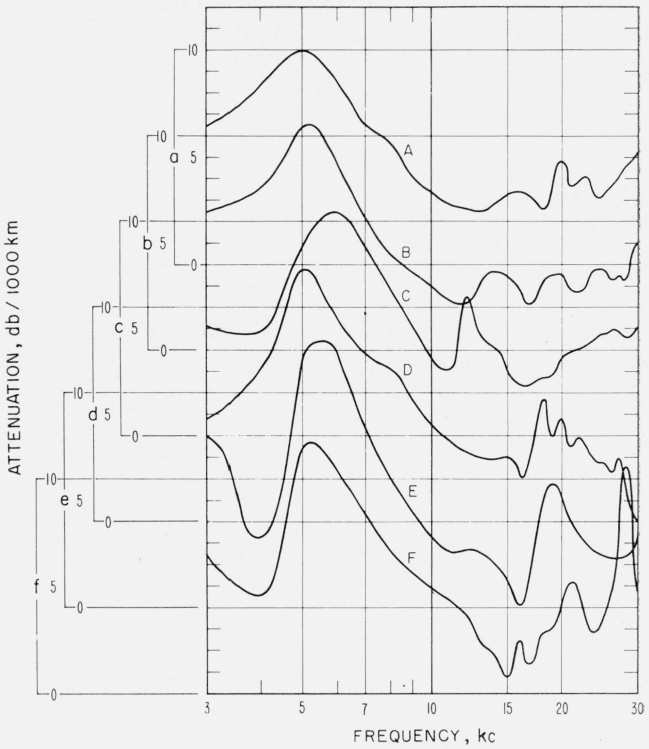

FIGURE 5. *Individual attenuation, east to west.*

A. Palo Alto, 1,040 km to Maui, 4,160 km.
B. Salt Lake City, 1,250 km to Maui, 4,480 km.
C. Salt Lake City, 1,470 km to Maui, 4,700 km.
D. Boulder, 1,650 km to Maui, 4,300 km.
E. Palo Alto, 1,840 km to Maui, 4,330 km.
F. Palo Alto, 2,000 km to Maui, 4,320 km.

figure. Variations of the computed attenuation about some mean value can be seen between 10 to 30 kc for each of these curves. The small, smooth variations of less than ± 1 db at frequencies above 10 kc, observed in curve B may well be produced by interference from higher order modes. Abrupt changes in attenuation, below 5 kc in all curves, and observed near 12 kc in curve C, 17 kc in curve D and E, and 29 kc in curve F, are most likely produced by various limitations in the recording and analysis techniques. These abrupt changes were observed only at those frequencies where the spectral amplitude component was extremely small for one or both of the waveforms recorded at a pair of stations. Small unwanted signals and noise, superimposed on the waveforms, and errors in tracing and scaling the waveforms may vary the resultant amplitude spectra by a few microvolt-seconds per meter (μvsec/m) at any frequency. Therefore, large errors would be expected at those frequencies where the computed amplitude of the spectra were small and therefore approaching the value introduced through limitations in the techniques.

Errors in the computed attenuation will tend toward a random distribution. Averaging the attenuation computed from a relatively large sample of independent data should give attenuation values that are reasonably accurate.

The average attenuation-versus-frequency values computed from the data recorded at each pair of stations are presented in figure 6. The average location of all lightning discharges used in this study was at 51°N to 118°W, i.e., the center of gravity for the discharges. The average distance from the lightning discharges was 1,220 km to Salt Lake City, 1,470 km to Palo Alto, 1,530 km to Boulder. All of these propagation paths occurred over land. The average distance to Maui was 4,580 km, which was all sea water except for 480 km at the source end of the average path. It can be seen from these distances that the average propagation path, over which these attenuation values were computed, was about 82 percent sea water for the Salt Lake City to Maui path, 76 percent sea water for the Palo Alto to Maui path, and 74 percent sea water for the Boulder to Maui path. The midpoint between this center or average location and Maui was approximately 34° N to 139° W where the direction of propagation was about 230° from geographic north.[3]

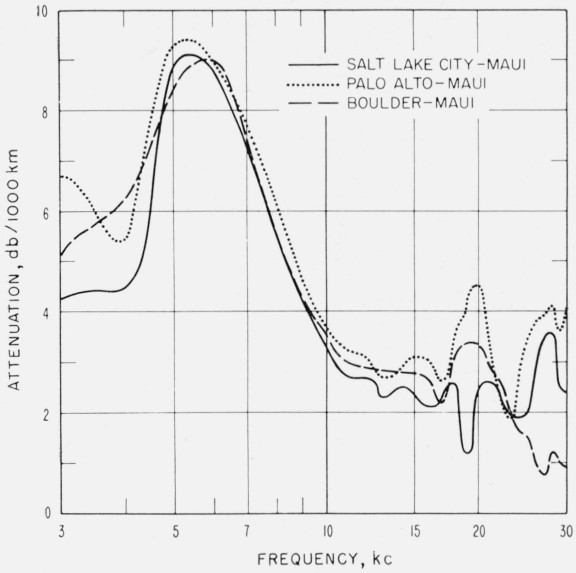

FIGURE 6. *Average attenuation by station, east to west.*

The average of the three curves is shown in figure 7. This curve represents experimentally-derived attenuation coefficients versus frequency for an approximately east-to-west path over predominantly sea-water conditions for summer, daytime conditions. The attenuation values represented by this curve may be low compared to an all sea-water path. An approximate correction to these values can be calculated by assuming the attenuation for a land path is 1 db greater for all frequencies than for a sea-water path. Using this approach, it can be shown that the attenuation values should be possibly increased by about 0.3 db/1,000 km.

3.3. Analysis—West-to-East Propagation

Attenuation coefficients for this study were computed from the data recorded at Maui and Palo Alto.

[3] Geomagnetic direction of propagation was about 215° and the dip angle of the earth's magnetic field was about 56°.

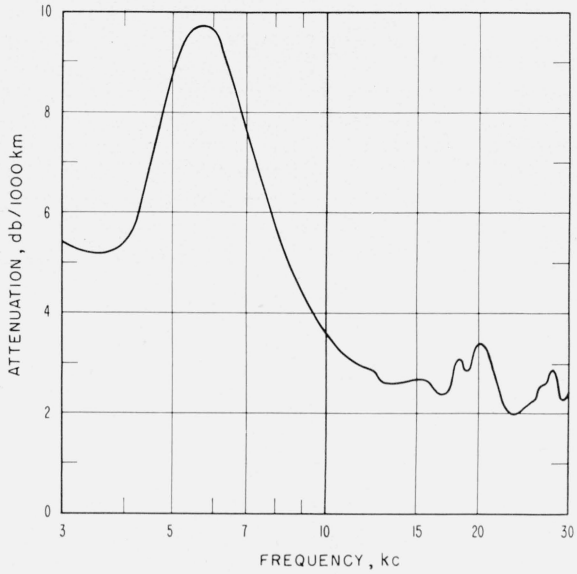

FIGURE 7. *Average daytime attenuation, east to west.*

Only one set of attenuation values were obtained from each lightning discharge, in which Maui was the close station and Palo Alto was the far station. The stations at Salt Lake City and Boulder did not record the atmospherics used in this part of the analysis because of the high level of atmospheric activity relatively near these stations during each observation period. Waveforms from 16 lightning discharges occuring in the western Pacific Ocean were obtained from the data collected on July 2, 1958, 1900 to 2100 G.m.t., and on July 9, 1958, 1900 to 2100 G.m.t. Eight of these were selected for the attenuation study.

Analysis of these data was conducted in the same manner as for the east-to-west attenuation computations. One pair of representative waveforms is shown in figure 8, reproduced on the same time base. Again the times of the zero-axis crossings of the Palo Alto waveform, recorded at the more distant station, are slightly less than for the Maui waveform.

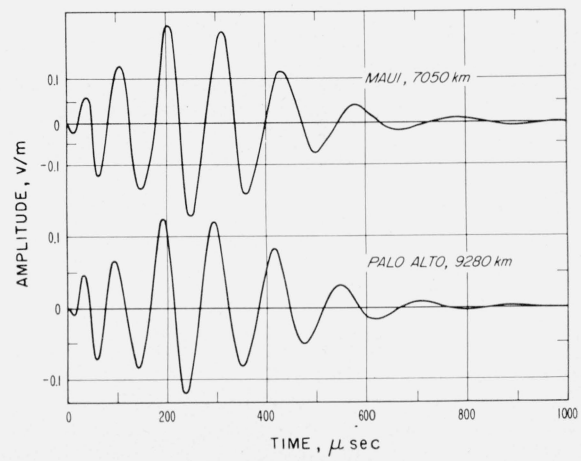

FIGURE 8. *Representative atmospheric waveforms, west to east.*

The spectra of these two atmospherics are presented in figure 9. The frequency of the peak amplitude of the Palo Alto spectrum occurs about 500 cycles higher than the corresponding peak of the Maui spectrum. Oscillations of the spectra, occurring between about 15 to 40 kc, are probably produced, at least in part, by an apparant "phase" shift in the waveform between the fifth and sixth half cycles as seen in figure 8. Phenomena of this type have been reported in the literature [9].

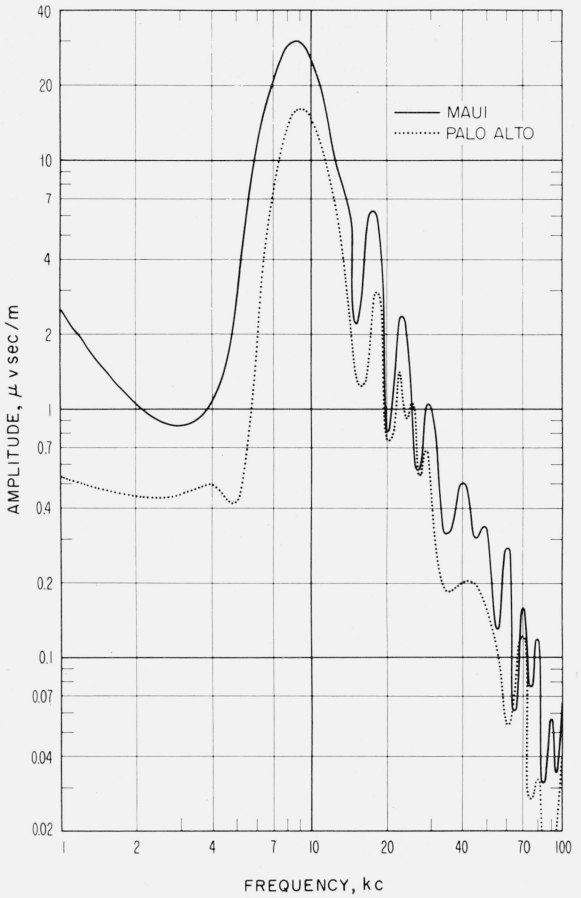

FIGURE 9. *Representative spectra, west to east.*

Attenuation in decibels per 1,000 km computed from this pair of atmospherics is shown in figure 10. Oscillations in the Palo Alto and Maui spectra, mentioned above, show their effect here as oscillations in the attenuation curve.

The average attenuation values, computed from the selected pairs of waveforms, are presented in figure 11. The accuracy of determining the location of individual atmospherics was about ±20 percent of the distance to the near station (Maui), but the accuracy of determining the differences in distance between each station and the source was about ±10 percent. Approximate average distance from the source to Maui was 6,460 km, and from the source to Palo Alto was 9,160 km. The midpoint between the center or average location of the discharges and

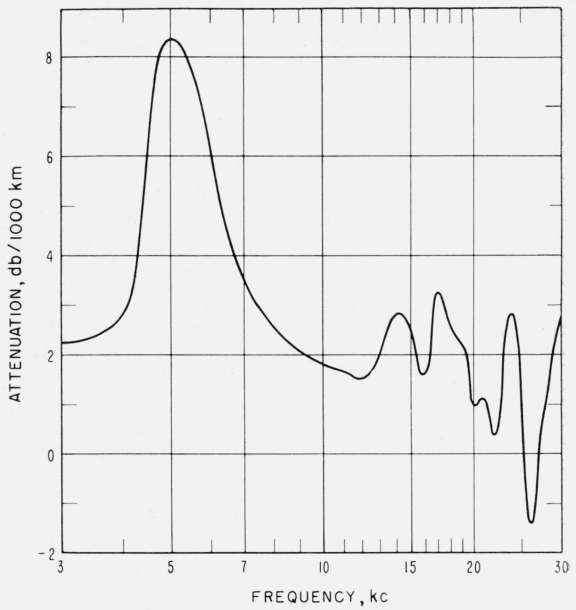

FIGURE 10. *Representative attenuation, west to east.*

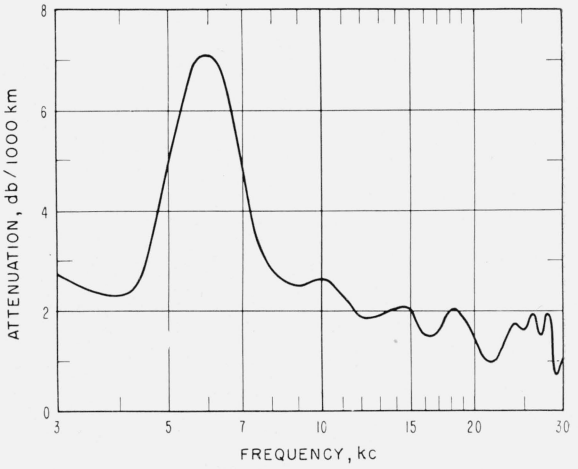

FIGURE 11. *Average daytime attenuation, west to east.*

Palo Alto was approximately 33° N to 176° W where the direction of propagation was about 68° from geographic north.[4] This curve represents experimentally derived attenuation coefficients versus frequency for an approximately west-to-east path, over sea water, for summer, daytime propagation.

4. Concluding Remarks

The general shape and the absolute values of the east-to-west attenuation-versus-frequency curve in figure 7 agrees reasonably well with the experimental and theoretical works of others.[5] The attenuation values for west-to-east propagation in figure 11 are somewhat lower than might be expected for a sharply bounded ionospheric model having reasonable values

[4] Geomagnetic direction of propagation was about 58° and the dip angle of the earth's magnetic field was about 49°.

[5] A selection of representative references is appended.

of reflection height, electron density, and collisional frequency. The differences between these two attenuation curves are shown in figure 12. This represents the attenuation for east-to-west propagation minus the attenuation for west-to-east propagation. A signal propagating from west to east is attenuated 3 db/1,000 km less between frequencies of about 3 to 8 kc, and 1 db/1,000 km less between frequencies of about 10 to 30 kc, than a signal propagating from east to west. The effect of a decreased attenuation at frequencies below about 8 kc would be to enhance the smooth oscillatory characteristics of atmospherics at great ranges. This characteristic has been observed by Hepburn [6] and by Chapman and Pierce [10] who reported the occurrence of long oscillatory, quasi-sinusoidal waveforms from a southwesterly direction.

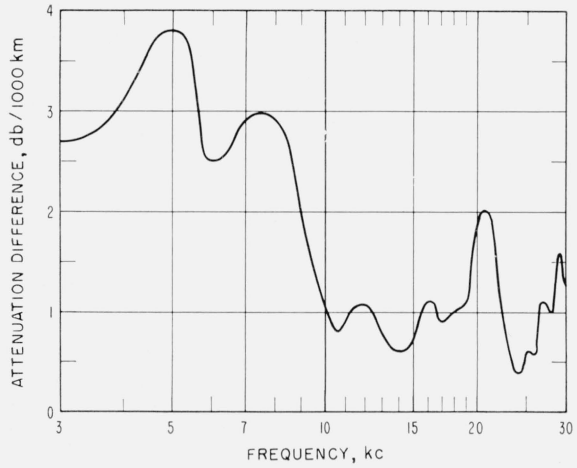

FIGURE 12. *Increased attenuation for east to west compared with west to east for daytime propagation.*

The 1 db/1,000 km difference in attenuation rates between 10 and 30 kc is also in agreement with various propagation studies using transmissions from VLF stations. Attenuation rates [11] computed from the data of Round et al. [12], indicate that propagation from east to west is characterized by an increase in attenuation of 1 or 2 db/1,000 km compared with propagation from west to east. Measurements of Heritage et al. [13], indicates that attenuation over the Pacific is slightly higher for east-to-west than for west-to-east propagation. Similar results were reported by Crombie [14].

It seems reasonable to conclude that propagation from west to east is better than from east to west. Much work remains to be done if this effect is to be understood fully. In particular, attenuation versus frequency should be determined as a function of the direction of propagation with respect to the earth's magnetic field lines. Theoretical investigations also should be extended to include those effects.

The author thanks C. Alley, University of Utah at Salt Lake City; W. Cornell, Stanford University at Palo Alto; C. Chilton, NBS at Boulder; S. Katahara, NBS at Maui; and all others who assisted in the collection of data for this paper. Also, the author thanks A. G. Jean and J. R. Wait for stimulating discussions on this subject, H. H. Howe who devised the program for the spectra computations, L. J. Lange and A. Murphy for further assistance with the computations, and Lois Pollock for computing attenuation values and preparing the illustrations.

5. References

[1] A. G. Jean, W. L. Taylor, and J. R. Wait, VLF phase characteristics deduced from atmospheric waveforms, J. Geophys. Research **65,** 907 (March 1960).
[2] J. R. Wait, The mode theory of VLF ionospheric propagation for finite ground conductivity, Proc. IRE **45,** 760 (1957).
[3] J. R. Wait, On the mode theory of VLF ionospheric propagation, Geofis. pura e appl. (Milano) **37,** 103 (1957).
[4] J. R. Wait, An extension to the mode theory of VLF ionospheric propagation, J. Geophys. Research **63,** 125 (1958).
[5] W. L. Taylor and L. J. Lange, Some characteristics of VLF propagation using atmospheric wave forms, Recent Adv. Atmos. Elec., p. 609 (Pergamon Press, Inc., New York, N.Y., (1959)).
[6] F. Hepburn, Wave-guide interpretation of atmospheric waveforms, J. Atmospheric and Terrest. Phys. **10,** 121 (1957).
[7] H. Norinder, The waveform of the electric field in atmospherics, Arkiv Geophys. **2,** 161 (1954).
[8] J. R. Wait, Propagation of VLF pulses to great distances, J. Research NBS **61,** 187 (1958) RP2898.
[9] F. Hepburn, Interpretation of smooth type atmospheric waveforms, J. Atmospheric and Terrest. Phys. **14,** 262 (1959).
[10] J. Chapman and E. T. Pierce, Relations between the character of atmospherics and their place of origin, Proc. IRE **45,** 804 (1957).
[11] J. R. Wait, A study of VLF field strength data, Geofis. pura e appl. **41,** 73 (1958).
[12] H. J. Round, T. L. Eckersley, K. Tremellen, and F. C. Lunnen, Report on measurements made on signal strength at great distances during 1922 and 1923 by an expedition sent to Australia, J. Inst. Elect. Engrs. **63,** 933 (1925).
[13] J. L. Heritage, S. Weisbrod, J. E. Bickel, A study of signal-vs-distance data at VLF Record Symp. on VLF propagation, Boulder, Colo. (Jan. 1957).
[14] D. D. Crombie, Differences between east-west and west-east propagation of VLF signals over long distances, J. Atmospheric and Terrest. Phys. **12,** 110 (1957).

Additional References

P. W. A. Bowe, The waveforms of atmospherics and the propagation of VLF radio waves, Phil. Mag. 42, 121 (1951).
K. G. Budden, On the propagation of a radio atmospheric, II, Phil. Mag. **43,** 1179 (1952).
F. W. Chapman and R. C. V. Macario, Propagation of audiofrequency radio waves to great distances, Nature **177,** 930 (1956).
W. L. Taylor and A. G. Jean, Very-low-frequency radiation spectra of lightning discharges, J. Research NBS **D63,** 199 (1959).
J. R. Wait, The attenuation vs frequency characteristics of VLF radio waves, Proc. IRE **45,** 768 (1957).
A. D. Watt and E. L. Maxwell, Characteristics of atmospheric noise from 1 to 100 kc, Proc. IRE **45,** 787 (1957).

(Paper 64D4–68)